HHS Public Access

Author manuscript

J Alzheimers Dis. Author manuscript; available in PMC 2024 July 23.

Published in final edited form as:

J Alzheimers Dis. 2024 ; 99(3): 1023–1032. doi:10.3233/JAD-240136.

TDP-43 Is Associated with Subiculum and Cornu Ammonis 1 Hippocampal Subfield Atrophy in Primary Age-Related Tauopathy

Hossam Youssef[a], **Rodolfo G. Gatto**[a], **Nha Trang Thu Pham**[b], **Ronald C. Petersen**[a], **Mary M. Machulda**[c], **R. Ross Reichard**[d], **Dennis W. Dickson**[e], **Clifford R. Jack**[b], **Jennifer L. Whitwell**[b], **Keith A. Josephs**[a,*]

[a]Department of Neurology, Mayo Clinic, Rochester, MN, USA

[b]Department of Radiology, Mayo Clinic, Rochester, MN, USA

[c]Department of Psychiatry & Psychology, Mayo Clinic, Rochester, MN, USA

[d]Laboratory Medicine and Pathology, Mayo Clinic, Rochester, MN, USA

[e]Department of Neuroscience (Neuropathology), Mayo Clinic, Jacksonville, FL, USA

Abstract

Background: TAR DNA binding protein 43 (TDP-43) has been shown to be associated with whole hippocampal atrophy in primary age-related tauopathy (PART). It is currently unknown which subregions of the hippocampus are contributing to TDP-43 associated whole hippocampal atrophy in PART.

Objective: To identify which specific hippocampal subfield regions are contributing to TDP-43-associated whole hippocampal atrophy in PART.

Methods: A total of 115 autopsied cases from the Mayo Clinic Alzheimer Disease Research Center, Neurodegenerative Research Group, and the Mayo Clinic Study of Aging were analyzed. All cases underwent antemortem brain volumetric MRI, neuropathological assessment of the distribution of Aβ (Thal phase), and neurofibrillary tangle (Braak stage) to diagnose PART, as well as assessment of TDP-43 presence/absence in the amygdala, hippocampus and beyond. Hippocampal subfield segmentation was performed using FreeSurfer version 7.4.1. Statistical

*Correspondence to: Keith A. Josephs, MD, MST, MSc, Professor of Neurology and Neuroscience, Ani Professor of Alzheimer's Disease Research, Behavioral Neurology and Movement Disorders, Department of Neurology, Mayo Clinic, College of Medicine, and Science, 200 First ST S.W., Rochester, MN 55902, USA. josephs.keith@mayo.edu.

AUTHOR CONTRIBUTIONS

Hossam Youssef (Conceptualization; Data curation; Formal analysis; Methodology; Project administration; Visualization; Writing – original draft); Rodolfo G. Gatto (Validation; Writing – review & editing); Nha Trang Thu Pham (Methodology; Resources; Software); Ronald C. Petersen (Validation; Writing – review & editing); Mary M. Machulda (Validation; Writing – review & editing); R. Ross Reichard (Validation); Dennis W. Dickson (Validation); Clifford R Jack (Validation; Writing – review & editing); Jennifer L. Whitwell (Conceptualization; Supervision; Validation; Writing – review & editing); Keith A. Josephs (Conceptualization; Methodology; Supervision; Validation; Writing – review & editing).

CONFLICT OF INTEREST

Jennifer Whitwell is an Editorial Board Member of this journal but was not involved in the peer-review process of this article nor had access to any information regarding its peer-review.

All other authors have no conflict of interest to report.

analyses using logistic regression were performed to assess for associations between TDP-43 and hippocampal subfield volumes, accounting for potential confounders.

Results: TDP-43 positive patients (n = 37, 32%), of which 15/15 were type-α, had significantly smaller whole hippocampal volumes, and smaller volumes of the body and tail of the hippocampus compared to TDP-43 negative patients. Subfield analyses revealed an association between TDP-43 and the molecular layer of hippocampal body and the body of cornu ammonis 1 (CA1), subiculum, and presubiculum regions. There was no association between TDP-43 stage and subfield volumes.

Conclusions: Whole hippocampal volume loss linked to TDP-43 in PART is mainly due to volume loss occurring in the molecular layer, CA1, subiculum and presubiculum of the hippocampal body.

Keywords

Alzheimer's disease; Cornu Ammonis 1; LATE-NC; primary age-related tauopathy; TAR DNA binding Protein 43; type-alpha

INTRODUCTION

Primary age-related tauopathy (PART) describes a pathology that combines a limbic predominant distribution of neurofibrillary tangles (NFTs) in the absence or limited distribution of amyloid-β (Aβ) [1]. PART is diagnosed when the Braak NFT stage [2] is I-V and the Aβ Thal phase is 0 (Definite PART) or Aβ Thal phase is 1–2 (Possible PART) [3]. PART has been associated with variable cognition ranging from normal cognition to dementia, with the latter previously being referred to as 'tangle-predominant senile dementia' (TPSD), 'tangle-only dementia', 'preferential development of NFT without senile plaques', and 'senile dementia of the neurofibrillary tangle type' (SD-NFT) [1]. Studies show that patients with PART have atrophy of the hippocampus which was presumed to be due to accumulation of the protein tau in the form of NFTs [4–6].

The transactive response DNA-binding protein of 43 kDa (TDP-43) is present in different neurodegenerative diseases. It was first linked to frontotemporal lobar degeneration and amyotrophic lateral sclerosis [7], but later was shown to be present in a significant percentage of cases of with Alzheimer's disease, as well as in other neurodegenerative diseases [8–10]; some researchers have advocated for the label limbic predominant age-related TDP-43 encephalopathy neuropathologic changes or LATE-NC [11]. In recent studies, we reported finding an association between TDP-43 and whole hippocampal volume loss in cases of PART [12, 13].

Studies on Alzheimer's disease have shown that TDP-43 is associated with volume loss of specific hippocampal subfields, which together contributes to whole hippocampal volume loss [2, 14, 15]. In addition, TDP-43 burden has been shown to be associated with inward deformation of the hippocampus in zones approximating CA1 and subiculum in AD [16]. In PART, similar to Alzheimer's disease [9, 17], TDP-43 pathology starts in the medial temporal lobe and progresses to the hippocampus and neocortex [2]. Although there are studies that have investigated the distribution and burden of TDP-43 pathology in

hippocampal subfields, volume loss in specific subfields of the hippocampus associated with TDP-43 in PART have not been investigated.

Consequently, the lack of knowledge of this relationship prompted us to investigate the associations between hippocampal subfields and TDP-43 in PART, to ascertain the specific hippocampal subfields that contribute to the association between TDP-43 and the overall loss of hippocampal volume. Results from this study will increase our understanding of TDP-43 and PART pathophysiology and highlight specific hippocampal subfields as potential targeted imaging biomarkers of TDP-43 pathology. We hypothesized that patients with PART and TDP-43 will exhibit smaller volumes in the CA1, subiculum and dentate gyrus of the hippocampus since these are the areas primarily affected by TDP-43 deposition.

METHODS

Study population

We identified 115 cases that met the criteria for possible or definite PART from a cohort of 1,720 autopsy confirmed cases who had been enrolled and followed longitudinally in the Mayo Clinic Alzheimer Disease Research Center, the Mayo Clinic Study of Aging (ADRC/MCSA), or the Neurodegenerative Research Group (NRG), completed at least one antemortem GE volumetric head MRI scan, died and underwent a comprehensive brain autopsy between January 1, 1999 and December 31, 2022. All MRI scans had been completed between this time period.

Pathological analyses

All 115 cases underwent standardized neuropathological examinations, including tissue sampling and semi-quantitative assessment of Alzheimer's disease pathology following the National Institute on Aging and Alzheimer's Association (NIA-AA) criteria [12, 13]. Each case was assigned a Braak NFT stage and a Thal Aβ stage in accordance with NIA-AA recommendations. Braak stages I and II correspond to NFT involvement primarily in the transentorhinal and entorhinal regions of the brain; Braak NFT stages III–IV are indicative of spread to the limbic regions, including the hippocampus; and Braak stages V–VI are characterized by extensive NFT involvement of the neocortex [2]. The Thal stages were utilized to categorize the distribution of Aβ deposition: Phase 0 = absence of Aβ throughout the entire brain; Phase 1 = presence of Aβ in the neocortex; Phase 2 presence of Aβ in allocortex/limbic areas; Phase 3 presence of Aβ in the diencephalon/basal ganglia; Phase 4 presence of Aβ in the brainstem/midbrain; and Phase 5 presence of Aβ in the cerebellum [18].

For this study we only included cases with Thal phases 0, 1, and 2, and Braak NFT stages I–IV which meets published inclusion criteria for PART [1, 3]. Hence, we excluded cases with Braak stage 0, V, and VI and Thal phase 3–5.

TDP-43 assessment

For all 115 cases, amygdala and hippocampal samples, from the left hemisphere, were sectioned and paraffin blocks created. The right hemisphere was frozen at the time of brain

harvesting. Blank slides were then immunostained to detect TDP-43 using a conformation specific antibody that recognizes the C-terminal fragment of TDP-43 (MC2085; gift from Leonard Petrucelli) [7]. Immunostaining was done using a DAKO-Autostainer machine with 3, 3′-diaminobenzidine as the color indicator following by the addition of a light Hematoxylin stain. Amygdala and hippocampal stained slides were examined by a neuropathologist (DWD) and neuroscientist (KAJ) to assess for the presence of TDP-43 immunoreactive inclusions and for TDP-43 type [19]. We focused on these two regions because we and others have previous shown that these two regions are affected early by TDP-43 in PART [9, 10]. Cases were reviewed at a magnification of 200X and were considered positive if any TDP-43 immunoreactive inclusion including neuronal cytoplasmic inclusions, dystrophic neurites, neuronal intranuclear inclusions, fine neurites of the CA-1 region of the hippocampus, NFT-associated TDP-43 (TATs) [20], perivascular and granular inclusions were observed [2, 9, 17]. If no TDP-43 was observed in either the amygdala or hippocampus, the case was designated TDP-negative. If TATs were the predominant lesion type or very prominent in the amygdala the case was labelled as TDP-43 type-beta [19]. However, if TATs were absent or relatively scant compared to the presence of neuronal cytoplasmic inclusions and/or dystrophic neurites, the case was labelled as TDP-43 type-alpha[19]. TDP-43 stage was also determined as previously described on a scale from stage 1 (amygdala only) – stage 6 (extending to frontal cortex or basal ganglia) [9, 17].

Brain MRI segmentation

In this study, we used the MRI scan nearest to the time of death in participants with multiple serial MRIs. All participants underwent a volumetric MRI using a standardized protocol [21], and all scans underwent correction for intensity inhomogeneity and were subjected to quality control for subsequent analysis. The segmentation of hippocampal subfields was performed using FreeSurfer version 7.4.1, which utilizes a probabilistic atlas constructed from ultra-high-resolution ex vivo MRI data (approximately 0.1 mm isotropic) to produce an automated segmentation of the hippocampal substructures [22, 23]. FreeSurfer subdivides hippocampal substructures into head, body, and tail, where applicable, and generates an additional set of segmentations of each hemisphere at different levels of hierarchy. This approach echoes historical methodologies, as delineated by an early foundational paper by Clifford et al., which pioneered the analysis of the hippocampus by its segmented region [24]. An example segmentation is shown in Figs. 1 and 2. Averaging the volumetric data of the left and right hippocampi has been utilized to reduce lateralization bias, to increase statistical power by reducing variability due to side-specific differences, and for a holistic representation of hippocampal volume changes. To adjust for differences in head size, total intracranial volume (TIV) was calculated using the standard FreeSurfer processing pipeline.

Statistical analysis

Statistical analysis was performed using STAT/BE 18, with significance set at a threshold of $p \leq 0.05$. Demographics, clinical characteristics, and MRI volumes of the patients were analyzed using basic descriptive statistics, including frequency, percent-age, mean, and standard deviation (SD). Differences between TDP-43 positive (+) and negative (−) cases were assessed by comparing the means and SDs of the two groups. Logistic regression was utilized to calculate the odds ratio for the association between TDP-43 positivity (dependent)

and hippocampal subfield volumes (independent), adjusting for TIV (independent). The Pearson correlation coefficient and one-way analysis of variance (ANOVA) were used to assess for correlations between TDP-43 stages and volumes. The Benjamini-Hochberg procedure was employed to control for a false discovery rate from performing multiple comparisons in our logistic regression analyses.

RESULTS

Demographic characteristics are displayed in Table 1. Of the 115 participants, approximately 43% were female. The average age at the time of their last MRI was 84 years, and the average age at death was 88 years. Thirty-seven participants were TDP-positive (32%). TDP-43 type was available for 15 participants in the TDP-43 positive group, and all were type-alpha. There was a significant difference observed between TDP-positive and negative groups in the frequency of hippocampal sclerosis ($p = 0.001$). Ten participants had hippocampal sclerosis (8.7%), with eight in the TDP-positive group (21.62%) and two in the TDP-negative group (2.56%). Both patients in the TDP-43 negative group had vascular lesions in the hippocampus. No significant differences were noted in the remaining demographic variables between TDP-positive and TDP-negative groups. There was a trend, however, for the TDP-43-positive group to be older at the time of death.

The findings for hippocampal volumes are shown in Table 2. Whole hippocampal volume was significantly smaller in the TDP-positive cases compared to the TDP-negative cases ($p = 0.049$). After stratification of the hippocampus into head, body, and tail, the TDP-positive cases showed smaller volumes of the hippocampal body ($p = 0.031$) and tail ($p = 0.021$), but not the hippocampal head ($p = 0.129$), compared to TDP-negative cases. When these regions were further subdivided into hippocampal subfields, the TDP-positive cases showed smaller volumes of molecular layer of hippocampal body ($p = 0.046$), CA1 body ($p = 0.031$), subiculum body ($p = 0.023$), as well as presubiculum body ($p = 0.046$) compared to TDP-negative cases. After separating definite from possible PART, no association was found between TDP-43 and volume in those with definite PART. TDP-43 staging was available for 32 participants of the TDP-43 positive group and there was no correlation found between staging and volumes of the whole hippocampi or subfields.

Results from the logistic regression analysis, are presented in Table 3. After adjusting for TIV, we found that reduced volumes of the whole hippocampus, hippocampal body, and its constituents including the molecular layer, CA1, subiculum and presubiculum had higher odds of being TDP-43 positive. After adjusting for hippocampal sclerosis, the results were essentially unchanged. TDP-43 remained associated with hippocampal body ($p = 0.046$), hippocampal tail ($p = 0.025$), CA1 body ($p = 0.041$), and subiculum body ($p = 0.036$), and approached significance with whole hippocampus ($p = 0.055$).

DISCUSSION

In this cohort of 115 cases of PART, we assessed the association of TDP-43 status with hippocampal subfield atrophy. We found that TDP-positive cases exhibited smaller whole hippocampal volumes compared to TDP-negative cases, validating our previous results [12,

13]. Further stratification revealed that the body and tail of the hippocampus showed smaller volumes in those with TDP-43. By further dissecting the hippocampus into subfields, we were able to attribute volume loss to the molecular layer of hippocampal body, CA1 body, subiculum body, and presubiculum body.

Our finding of smaller whole hippocampal volume in TDP-positive cases with PART concurs with our previous studies demonstrating the influence of TDP-43 on brain volumes in PART [12, 13]. In this study, we further investigate the specific regions and subfields of the hippocampus and discovered that differences in volume loss are more prominent in the body and tail of the hippocampus in the TDP-positive cases. Moreover, with further stratification and analysis, volume loss was observed in the molecular layer of hippocampal body, CA1 body, subiculum body, as well as presubiculum body. To our knowledge, this is the first study to investigate the effects of TDP-43 in patients with PART on hippocampal subfields. Based on the FreeSurfer anatomical atlas [22], we note that the hippocampal tail has no subfield components. However, the body is comprised of various components, including the molecular layer, CA1, subiculum, and presubiculum, which are all significantly smaller in volume in TDP-positive cases. Notably, the same effect was not observed in absence of beta-amyloid which is consistent with our previous study that also found no association between TDP-43 and whole hippocampal volumes in patients with definite PART [5]. This is likely because the vast majority of patients with definite PART are cognitively normal with absent to minimal volume loss, and no range of data for volumes. We did observe a trend for the volume of the head of the hippocampus to be smaller in the TDP-positive cases compared to the TDP-43 negative cases.

In neuropathological studies where TDP-43 pathology has been observed, there is significant deposition of TDP-43 in regions and subregions of medial temporal lobe structures including the CA1 and subiculum regions of the hippocampus [25]. TDP-43 has been previously found to have an effect on the hippocampal subfields CA1 and subiculum in Alzheimer’s disease and has been associated with inward deformation of the hippocampus, which correlates with cognition scores [14]. It is not surprising that these two regions show volume loss associated with TDP-43 in Alzheimer’s disease and now in PART, because these two regions are directly affected by TDP-43 deposition [17]. In PART, however, it is vulnerability of the CA2 subregion due to NFT degeneration that is greatest [4, 26]. Our findings therefore are more keeping with volume loss due to TDP-43 than volume loss due to NFTs and tau.

We discovered that TDP-43 in PART predominantly impacts the hippocampal body, specifically affecting four main areas: the molecular layer, CA1, subiculum, and presubiculum. Given the observed volume loss in these areas, it may be worth exploring their potential as imaging biomarkers for TDP-43 associated atrophy in future longitudinal studies. However, the long-term performance and reliability of these biomarkers remain to be established through comprehensive research. Differential atrophy of the CA1 versus CA2 regions of the hippocampus could be utilized to assess treatment response to a tau versus TDP-43 targeted pharmacological molecule.

The CA1 and subiculum are also involved in hippocampal atrophy in Alzheimer’s disease where both Aβ and tau are present [27–29]. In individuals with Alzheimer’s disease,

reduced volumes of both CA1 and subiculum have been observed, consistent with atrophy in these two subfields [30]. Given that we have demonstrated a similar pattern of involvement in PART that is related to TDP-43, one could hypothesize that it is TDP-43 that is possibly driving atrophy in these two subfields in Alzheimer's disease. It is unclear however, whether there are differences between TDP-43 related subfield volume loss in Alzheimer's disease and TDP-43 related subfield volume loss in PART. For example, our analysis suggests more specific involvement of these regions in the body of the hippocampus as opposed to the head. It is possible that the hippocampal head is more affected than the body in Alzheimer's disease.

Unlike the CA1 and subiculum which have been discussed in previous studies, less is known about the molecular layer. In one study comparing the volume of the molecular layer in cognitively intact versus mild cognitively impaired patients, no significant difference was observed [31]. Similarly, little has been reported on the presubiculum in the body of the hippocampus.

There is a strong association between TDP-43 pathology and hippocampal sclerosis, with hippocampal sclerosis conceptualized as a downstream consequence of the presence of TDP-43 [32]. Hence, it is not surprising that those with TDP-43 were more likely to have hippocampal sclerosis compared to those without TDP-43. Unlike hippocampal sclerosis, there was no difference in the Braak NFT stage or the Thal phase between those with and without TDP-43. This is most likely due to the fact that our inclusion criteria limited cases to specific Braak and Thal stages. It is well known that patients with TDP-43 have higher Braak NFT stages when the full spectrum of Braak stage cases (I–VI) are included in the study [33, 34].

Strengths and limitations

One of the strengths of our study is the large sample size. In fact, to the best of our knowledge, this is the largest cohort to investigate the association between TDP-43 and hippocampal subfields in patients with PART. Another strength is that our cases were well characterized pathologically. Our study has certain limitations that warrant discussion. First, although segmenting the hippocampus into head, body, and tail provides more precision than analyzing the whole hippocampus, some subfield volumes are too small for accurate measurement using T1-weighted MRI. Consequently, the accuracy of some of our segmentations is likely poorer compared to larger parcellations. We also recognize that the hippocampal subfields lack distinct internal contrast in these roughly 1 mm clinical resolution T1-weighted MRI scans, resulting in the subfield segmentations being largely dependent on external atlas priors. In future studies, this limitation could be addressed by incorporating T2-weighted MRI [22]. Thirdly, the low odds ratios observed in our logistic regression model suggest that the differences in brain volume identified are small and may be influenced by other external factors. Fourth, we only identified one unaffected control case that was without PART and TDP-43 and had an antemortem GE MRI scan; therefore, we were unable to compare PART participants who were TDP-43 negative with unaffected control cases. Lastly, we were unable to assess difference by TDP-43 type as all cases were

TDP-43 type-alpha. This is not surprising since TDP-43 type-beta is associated with high Braak NFT stages [19] and the cases in this study with PART were Braak NFT stages ≤ IV.

Conclusion

In conclusion, our study underscores the association between TDP-43 pathology and hippocampal subfields in PART. It highlights which subfields are contributing to whole hippocampal volume loss, and particularly implicate the body and tail regions and specifically volumetric loss to the subfields of the CA1 and subiculum in the body.

ACKNOWLEDGMENTS

We would like to thank Ms. Monica Castanedes for performing the TDP-43 immunohistochemistry and Dr. Leonard Petrucelli for giving us the TDP-43 antibodies that were used in this study.

FUNDING

This study was funded by NIH grants R01 AG37491 (PI: Josephs), P50 AG16574 (PI: Petersen) and U01 AG006786 (PI: Petersen).

DATA AVAILABILITY

The data that support the findings of this study are available upon reasonable request to the corresponding authors (KAJ).

REFERENCES

[1]. Crary JF, Trojanowski JQ, Schneider JA, Abisambra JF, Abner EL, Alafuzoff I, Arnold SE, Attems J, Beach TG, Bigio EH, Cairns NJ, Dickson DW, Gearing M, Grinberg LT, Hof PR, Hyman BT, Jellinger K, Jicha GA, Kovacs GG, Knopman DS, Kofler J, Kukull WA, Mackenzie IR, Masliah E, McKee A, Montine TJ, Murray ME, Neltner JH, Santa-Maria I, Seeley WW, Serrano-Pozo A, Shelanski ML, Stein T, Takao M, Thal DR, Toledo JB, Troncoso JC, Vonsattel JP, White CL 3rd, Wisniewski T, Woltjer RL, Yamada M, Nelson PT (2014) Primary age-related tauopathy (PART): A common pathology associated with human aging. Acta Neuropathol 128, 755–766. [PubMed: 25348064]

[2]. Zhang X, Sun B, Wang X, Lu H, Shao F, Rozemuller AJM, Liang H, Liu C, Chen J, Huang M, Zhu K (2019) Phosphorylated TDP-43 staging of primary age-related tauopathy. Neurosci Bull 35, 183–192. [PubMed: 30382507]

[3]. Kim D, Kim HS, Choi SM, Kim BC, Lee MC, Lee KH, Lee JH (2019) Primary age-related tauopathy: An elderly brain pathology frequently encountered during autopsy. J Pathol Transl Med 53, 159–163. [PubMed: 30887795]

[4]. Walker JM, Richardson TE, Farrell K, Iida MA, Foong C, Shang P, Attems J, Ayalon G, Beach TG, Bigio EH, Budson A, Cairns NJ, Corrada M, Cortes E, Dickson DW, Fischer P, Flanagan ME, Franklin E, Gearing M, Glass J, Hansen LA, Haroutunian V, Hof PR, Honig L, Kawas C, Keene CD, Kofler J, Kovacs GG, Lee EB, Lutz MI, Mao Q, Masliah E, McKee AC, McMillan CT, Mesulam MM, Murray M, Nelson PT, Perrin R, Pham T, Poon W, Purohit DP, Rissman RA, Sakai K, Sano M, Schneider JA, Stein TD, Teich AF, Trojanowski JQ, Troncoso JC, Vonsattel JP, Weintraub S, Wolk DA, Woltjer RL, Yamada M, Yu L, White CL, Crary JF (2021) Early selective vulnerability of the CA2 hippocampal subfield in primary age-related tauopathy. J Neuropathol Exp Neurol 80, 102–111. [PubMed: 33367843]

[5]. Josephs KA, Murray ME, Tosakulwong N, Whitwell JL, Knopman DS, Machulda MM, Weigand SD, Boeve BF, Kantarci K, Petrucelli L, Lowe VJ, Jack CR Jr., Petersen RC, Parisi JE, Dickson DW (2017) Tau aggregation influences cognition and hippocampal atrophy in the absence of

beta-amyloid: A clinico-imaging-pathological study of primary age-related tauopathy (PART). Acta Neuropathol 133, 705–715. [PubMed: 28160067]

[6]. Tetlow AM, Jackman BM, Alhadidy MM, Muskus P, Morgan DG, Gordon MN (2023) Neural atrophy produced by AAV tau injections into hippocampus and anterior cortex of middle-aged mice. Neurobiol Aging 124, 39–50. [PubMed: 36739619]

[7]. Zhang YJ, Xu YF, Cook C, Gendron TF, Roettges P, Link CD, Lin WL, Tong J, Castanedes-Casey M, Ash P, Gass J, Rangachari V, Buratti E, Baralle F, Golde TE, Dickson DW, Petrucelli L (2009) Aberrant cleavage of TDP-43 enhances aggregation and cellular toxicity. Proc Natl Acad Sci U S A 106, 7607–7612. [PubMed: 19383787]

[8]. Josephs KA, Dickson DW, Tosakulwong N, Weigand SD, Murray ME, Petrucelli L, Liesinger AM, Senjem ML, Spychalla AJ, Knopman DS, Parisi JE, Petersen RC, Jack CR Jr., Whitwell JL (2017) Rates of hippocampal atrophy and presence of post-mortem TDP-43 in patients with Alzheimer's disease: A longitudinal retrospective study. Lancet Neurol 16, 917–924. [PubMed: 28919059]

[9]. Josephs KA, Murray ME, Whitwell JL, Parisi JE, Petrucelli L, Jack CR, Petersen RC, Dickson DW (2014) Staging TDP-43 pathology in Alzheimer's disease. Acta Neuropathol 127, 441–450. [PubMed: 24240737]

[10]. Hu WT, Josephs KA, Knopman DS, Boeve BF, Dickson DW, Petersen RC, Parisi JE (2008) Temporal lobar predominance of TDP-43 neuronal cytoplasmic inclusions in Alzheimer disease. Acta Neuropathol 116, 215–220. [PubMed: 18592255]

[11]. Nelson PT, Dickson DW, Trojanowski JQ, Jack CR, Boyle PA, Arfanakis K, Rademakers R, Alafuzoff I, Attems J, Brayne C, Coyle-Gilchrist ITS, Chui HC, Fardo DW, Flanagan ME, Halliday G, Hokkanen SRK, Hunter S, Jicha GA, Katsumata Y, Kawas CH, Keene CD, Kovacs GG, Kukull WA, Levey AI, Makkinejad N, Montine TJ, Murayama S, Murray ME, Nag S, Rissman RA, Seeley WW, Sperling RA, White CL 3rd, Yu L, Schneider JA (2019) Limbic-predominant age-related TDP-43 encephalopathy (LATE): Consensus working group report. Brain 142, 1503–1527. [PubMed: 31039256]

[12]. Josephs KA, Martin PR, Weigand SD, Tosakulwong N, Buciuc M, Murray ME, Petrucelli L, Senjem ML, Spychalla AJ, Knopman DS, Boeve BF, Petersen RC, Parisi JE, Dickson DW, Jack CR, Whitwell JL (2020) Protein contributions to brain atrophy acceleration in Alzheimer's disease and primary age-related tauopathy. Brain 143, 3463–3476. [PubMed: 33150361]

[13]. Josephs KA, Murray ME, Tosakulwong N, Weigand SD, Knopman DS, Petersen RC, Jack CR Jr., Whitwell JL, Dickson DW (2019) Brain atrophy in primary age-related tauopathy is linked to transactive response DNA-binding protein of 43 kDa. Alzheimers Dement 15, 799–806. [PubMed: 31056344]

[14]. Heywood A, Stocks J, Schneider JA, Arfanakis K, Bennett DA, Beg MF, Wang L (2022) The unique effect of TDP-43 on hippocampal subfield morphometry and cognition. Neuroimage Clin 35, 103125. [PubMed: 36002965]

[15]. Wisse LEM, Ravikumar S, Ittyerah R, Lim S, Lane J, Bedard ML, Xie L, Das SR, Schuck T, Grossman M, Lee EB, Tisdall MD, Prabhakaran K, Detre JA, Mizsei G, Trojanowski JQ, Artacho-Perula E, de Iniguez de Onzono Martin MM, MA-J M, Munoz Lopez M, FJ Molina Romero, PMR M, Cebada Sanchez S, Delgado Gonzalez JC, de la Rosa Prieto C, Corcoles Parada M, Wolk DA, Irwin DJ, Insausti R, Yushkevich PA (2021) Downstream effects of polypathology on neurodegeneration of medial temporal lobe subregions. Acta Neuropathol Commun 9, 128. [PubMed: 34289895]

[16]. Hanko V, Apple AC, Alpert KI, Warren KN, Schneider JA, Arfanakis K, Bennett DA, Wang L (2019) In vivo hippocampal subfield shape related to TDP-43, amyloid beta, and tau pathologies. Neurobiol Aging 74, 171–181. [PubMed: 30453234]

[17]. Josephs KA, Murray ME, Whitwell JL, Tosakulwong N, Weigand SD, Petrucelli L, Liesinger AM, Petersen RC, Parisi JE, Dickson DW (2016) Updated TDP-43 in Alzheimer's disease staging scheme. Acta Neuropathol 131, 571–585. [PubMed: 26810071]

[18]. Thal DR, Rub U, Orantes M, Braak H (2002) Phases of A beta-deposition in the human brain and its relevance for the development of AD. Neurology 58, 1791–1800. [PubMed: 12084879]

[19]. Josephs KA, Murray ME, Tosakulwong N, Weigand SD, Serie AM, Perkerson RB, Matchett BJ, Jack CR Jr., Knopman DS, Petersen RC, Parisi JE, Petrucelli L, Baker M, Rademakers

R, Whitwell JL, Dickson DW (2019) Pathological, imaging and genetic characteristics support the existence of distinct TDP-43 types in non-FTLD brains. Acta Neuropathol 137, 227–238. [PubMed: 30604226]

[20]. Josephs KA, Koga S, Tosakulwong N, Weigand SD, Nha Pham TT, Baker M, Whitwell JL, Rademakers R, Petrucelli L, Dickson DW (2023) Molecular fragment characteristics and distribution of tangle associated TDP-43 (TATs) and other TDP-43 lesions in Alzheimer's disease. Free Neuropathol 4, 4–22.

[21]. Jack CR Jr., Lowe VJ, Senjem ML, Weigand SD, Kemp BJ, Shiung MM, Knopman DS, Boeve BF, Klunk WE, Mathis CA, Petersen RC (2008) 11C PiB and structural MRI provide complementary information in imaging of Alzheimer's disease and amnestic mild cognitive impairment. Brain 131, 665–680. [PubMed: 18263627]

[22]. Iglesias JE, Augustinack JC, Nguyen K, Player CM, Player A, Wright M, Roy N, Frosch MP, McKee AC, Wald LL, Fischl B, Van Leemput K, Alzheimer's Disease Neuroimaging I (2015) A computational atlas of the hippocampal formation using ex vivo, ultra-high resolution MRI: Application to adaptive segmentation of in vivo MRI. Neuroimage 115, 117–137. [PubMed: 25936807]

[23]. Iglesias JE, Van Leemput K, Augustinack J, Insausti R, Fischl B, Reuter M, Alzheimer's Disease Neuroimaging Initiative (2016) Bayesian longitudinal segmentation of hippocampal substructures in brain MRI using subject-specific atlases. Neuroimage 141, 542–555. [PubMed: 27426838]

[24]. Jack CR Jr., Petersen RC, Xu YC, Waring SC, O'Brien PC, Tangalos EG, Smith GE, Ivnik RJ, Kokmen E (1997) Medial temporal atrophy on MRI in normal aging and very mild Alzheimer's disease. Neurology 49, 786–794. [PubMed: 9305341]

[25]. Smirnov DS, Salmon DP, Galasko D, Edland SD, Pizzo DP, Goodwill V, Hiniker A (2022) TDP-43 pathology exacerbates cognitive decline in primary age-related tauopathy. Ann Neurol 92, 425–438. [PubMed: 35696592]

[26]. Morris M, Coste GI, Redding-Ochoa J, Guo H, Graves AR, Troncoso JC, Huganir RL (2023) Hippocampal synaptic alterations associated with tau pathology in primary age-related tauopathy. J Neuropathol Exp Neurol 82, 836–844. [PubMed: 37595576]

[27]. Kannappan B, Gunasekaran TI, Te Nijenhuis J, Gopal M, Velusami D, Kothandan G, Lee KH, Alzheimer's Disease Neuroimaging Initiative (2022) Polygenic score for Alzheimer's disease identifies differential atrophy in hippocampal subfield volumes. PLoS One 17, e0270795. [PubMed: 35830443]

[28]. Low A, Foo H, Yong TT, Tan LCS, Kandiah N (2019) Hippocampal subfield atrophy of CA1 and subicular structures predict progression to dementia in idiopathic Parkinson's disease. J Neurol Neurosurg Psychiatry 90, 681–687. [PubMed: 30683708]

[29]. Parker TD, Slattery CF, Yong KXX, Nicholas JM, Paterson RW, Foulkes AJM, Malone IB, Thomas DL, Cash DM, Crutch SJ, Fox NC, Schott JM (2019) Differences in hippocampal subfield volume are seen in phenotypic variants of early onset Alzheimer's disease. Neuroimage Clin 21, 101632. [PubMed: 30558867]

[30]. de Flores R, La Joie R, Chetelat G (2015) Structural imaging of hippocampal subfields in healthy aging and Alzheimer's disease. Neuroscience 309, 29–50. [PubMed: 26306871]

[31]. Scheff SW, Price DA, Schmitt FA, Mufson EJ (2006) Hippocampal synaptic loss in early Alzheimer's disease and mild cognitive impairment. Neurobiol Aging 27, 1372–1384. [PubMed: 16289476]

[32]. Yang HS, Yu L, White CC, Chibnik LB, Chhatwal JP, Sperling RA, Bennett DA, Schneider JA, De Jager PL (2018) Evaluation of TDP-43 proteinopathy and hippocampal sclerosis in relation to APOE epsilon4 haplotype status: A community-based cohort study. Lancet Neurol 17, 773–781. [PubMed: 30093249]

[33]. Josephs KA, Whitwell JL, Weigand SD, Murray ME, Tosakulwong N, Liesinger AM, Petrucelli L, Senjem ML, Knopman DS, Boeve BF, Ivnik RJ, Smith GE, Jack CR Jr., Parisi JE, Petersen RC, Dickson DW (2014) TDP-43 is a key player in the clinical features associated with Alzheimer's disease. Acta Neuropathol 127, 811–824. [PubMed: 24659241]

[34]. Tome SO, Tsaka G, Ronisz A, Ospitalieri S, Gawor K, Gomes LA, Otto M, von Arnim CAF, Van Damme P, Van Den Bosch L, Ghebremedhin E, Laureyssen C, Sleegers K, Vandenberghe R,

Rousseau F, Schymkowitz J, Thal DR (2023) TDP-43 pathology is associated with increased tau burdens and seeding. Mol Neurodegener 18, 71. [PubMed: 37777806]

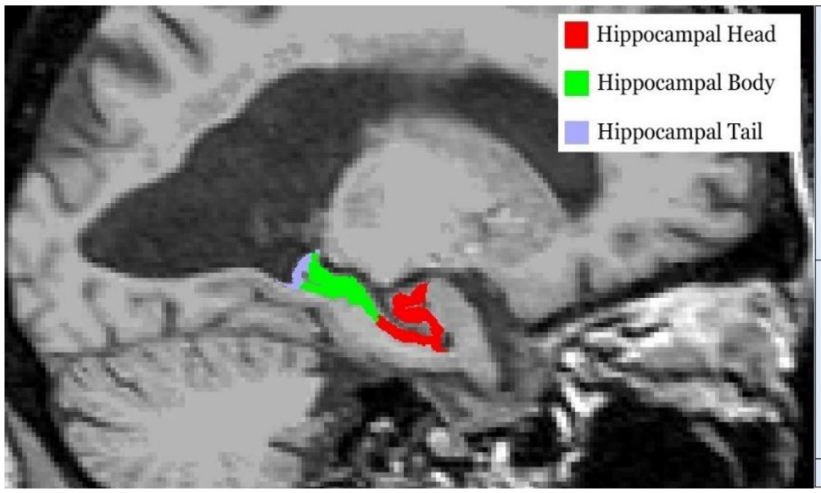

Hippocampal Head	Parasubiculum
	Presubiculum head
	Subiculum head
	CA1 head
	CA2/3 head
	CA4 head
	GC-ML-DG head
	Molecular layer
	HATA
Hippocampal Body	Presubiculum body
	Subiculum body
	CA1 body
	CA2/3 body
	CA4 body
	GC-ML-DG body
	Molecular layer
Hippocampal Tail	Tail

Fig. 1.

Hippocampal subfields' sagittal view. GC-ML-DG, Granule Cell and Molecular Layers of the Dentate Gyrus; HATA, Hippocampal-Amygdala Transition Area.

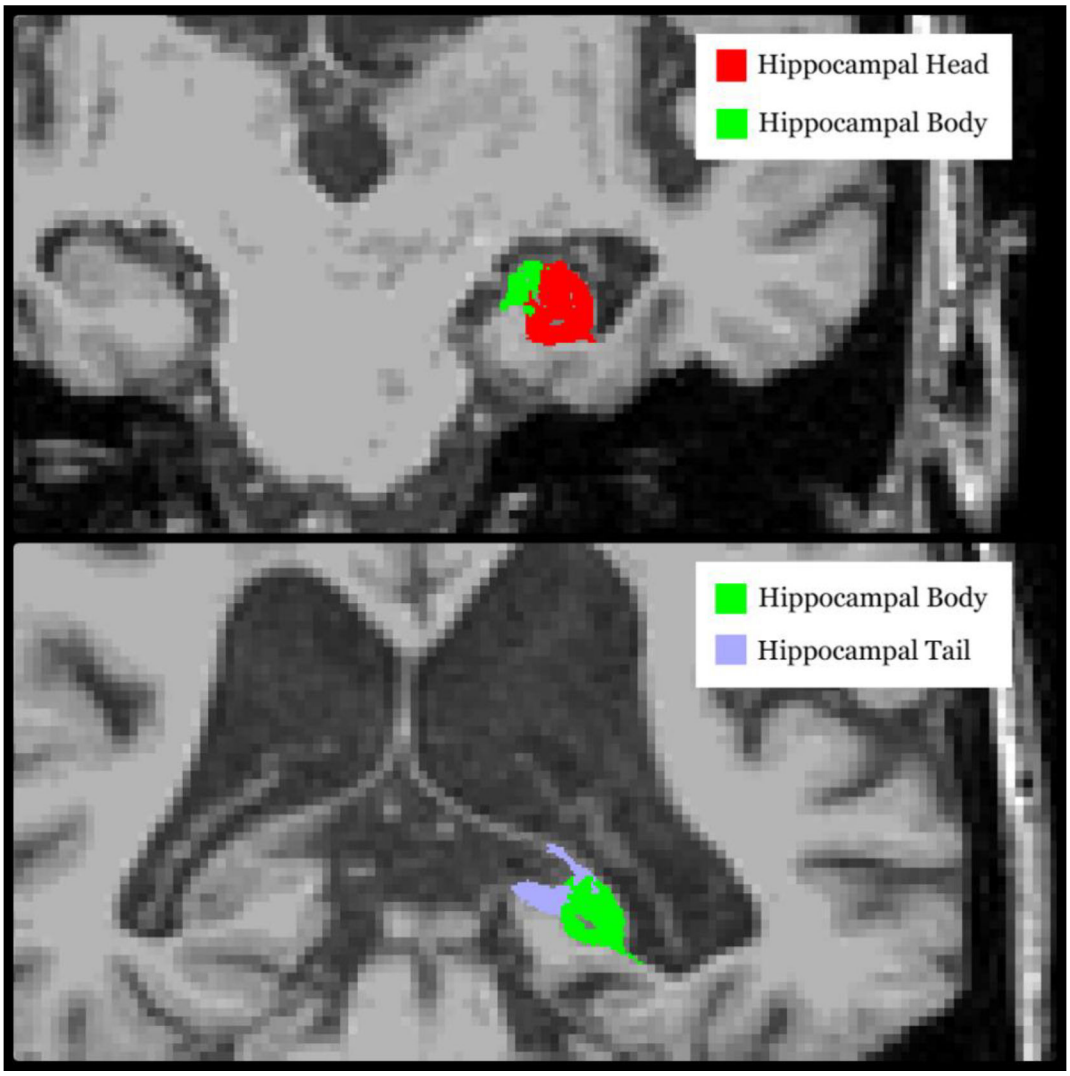

Fig. 2.
Hippocampal subfields' coronal view.

Table 1.

Participant characteristics.

Characteristics	Cohort (n=115)	TDP-negative (n=78)	TDP-positive (n=37)	p-value
Female sex, N (%)	49 (42.61%)	31 (39.74%)	18 (48.65%)	0.367
APOE4 carrier	20 (17.39%)	15 (19.23%)	5 (13.51%)	0.450
Age at last scan, years	84 (±6.3)	83.4 (±6.8)	85.4 (±4.6)	0.097
TIV $\times 10^5$	15.4 (±1.9)	15.5 (±1.9)	15.2 (±1.9)	0.401
Age at death, years	88.4 (±6.9)	87.6 (±7.4)	90.2 (±5.2)	0.052
Last scan to death, years	4.4 (±2.8)	4.2 (±2.7)	4.8 (±3)	0.296
MMSE	25 (±5)	25 (±6)	25 (±4)	0.562
CDR-SB	3.7 (±5.6)	3.3 (±5.5)	1.6 (±2.9)	0.081
WMS-R LM1	12.3 (± 12.2)	11.9 (±11.8)	14.2 (±12.9)	0.345
AVLT – half hour delay	0.22 (±1.8)	0.4 (±2.4)	0 (±0)	0.334
Hippocampal sclerosis, N (%)	10 (8.7%)	2 (2.56%)	8 (21.62)	0.001
Thal stage				0.114
0	44 (38.26%)	26 (33.33%)	18 (48.65%)	
1/2	73 (61.74%)	52 (66.67%)	19 (51.35%)	
Braak stage				0.885
I	14 (12.17%)	9 (11.54%)	5 (13.51%)	
II	35 (30.43%)	25 (32.05%)	10 (27.03%)	
III	45 (39.13%)	29 (37.18%)	16 (43.24%)	
IV	21 (18.26%)	15 (19.23%)	6 (16.22%)	

Data is shown as mean (±standard deviation) or N (%). Abbreviations: AVLT, Auditory Verbal Learning Test; CDR-SB, Clinical Dementia Rating Scale - Sum of Boxes; TIV, Total Intracranial Volume; MMSE, Mini-Mental State Examination; WMS-R LM1, Wechsler Memory Scale-Revised Logical Memory I.

Table 2.

Hippocampal volume findings across TDP-43 status groups

Hippocampal regions	TDP-negative (n=78)	TDP-positive (n=37)	p-value
Whole hippocampus	188 ±27	176 ±31	0.049
Hippocampal subdivisions			
Hippocampal head	93.0 ±14.5	88.4 ±16.8	0.129
Hippocampal body	63.1 ±9.6	58.8 ±10.2	0.031
Hippocampal tail	32.0 ±5.0	29.6 ±5.5	0.021
Hippocampal subfields			
Molecular layer of hippocampal head	18.2 ±3.0	17.2 ±3.6	0.116
Molecular layer of hippocampal body	12.1 ±2.1	11.3 ±2.2	0.046
GC-ML-DG head	8.5 ±1.5	7.9 ±1.6	0.122
GC-ML-DG body	7.6 ±1.3	7.3 ±1.2	0.129
CA4 head	7.4 ±1.2	7.0 ±1.4	0.137
CA4 body	7.3 ±1	6.9 ±1.6	0.144
CA2/3 head	6.5 ±1.3	6.4 ±1.4	0.166
CA2/3 body	5.2 ±1.2	4.9 ±1.0	0.229
CA1 head	28.4 ±4.6	26.7 ±4.9	0.091
CA1 body	6.6 ±1.1	6.1 ±1.2	0.031
Subiculum head	10.1 ±1.7	9.5 ±2/3	0.169
Subiculum body	12.9 ±2.1	11.9 ±2.5	0.023
Presubiculum head	7.2 ±1.4	6.8 ±1.8	0.279
Presubiculum body	8.4 ±1.6	7.7 ±1.8	0.046
Parasubiculum	3.8 ±0.9	3.9 ±1.0	0.614
HATA	2.9 ±0.7	2.9 ±0.6	0.795

Data is shown as mean (±standard deviation). Statistical analysis performed after adjusting for total intracranial volume.

Abbreviations: GC-ML-DG, Granule Cell and Molecular Layers of the Dentate Gyrus; HATA, Hippocampal-Amygdala Transition Area. Unitless normalized volumes are calculated as the ratio of hippocampal volumes to total intracranial volume, multiplied by 100,000.

Table 3.

Odds ratio of being TDP-43 positive.

ROI	odds ratio	95% conf. interval	p-value
Whole hippocampus	0.99	0.99–1	0.027
Hippocampal head	0.99	0.99–1	0.081
Hippocampal body	0.99	0.99–1	0.043
Hippocampal tail	0.99	0.99–1	0.072
Molecular layer of hippocampal head	0.99	0.98–1	0.075
Molecular layer of hippocampal body	0.99	0.97–1	0.033
CA1 head	0.99	0.99–1	0.066
CA1 body	0.97	0.94–0.99	0.030
Subiculum head	0.99	0.97–1	0.099
Subiculum body	0.98	0.97–1	0.043
Presubiculum head	0.99	0.97–1	0.144
Presubiculum body	0.98	0.96–1	0.030

Statistical analysis performed with logistic regression adjusted for total intracranial volume. P-values were corrected for false discovery rates (FDR) by employing the Benjamini-Hochberg procedure.